MEASLES

Measles virus and rinderpest virus divergence dated to the sixth century BCE

Ariane Düx[1,2]*, Sebastian Lequime[3]*, Livia Victoria Patrono[1,2], Bram Vrancken[3], Sengül Boral[4], Jan F. Gogarten[1,2], Antonia Hilbig[1], David Horst[4], Kevin Merkel[1,2], Baptiste Prepoint[2,5], Sabine Santibanez[6], Jasmin Schlotterbeck[2], Marc A. Suchard[7,8,9], Markus Ulrich[1], Navena Widulin[10], Annette Mankertz[6], Fabian H. Leendertz[1], Kyle Harper[11], Thomas Schnalke[10], Philippe Lemey[3]†, Sébastien Calvignac-Spencer[1,2]†‡

Many infectious diseases are thought to have emerged in humans after the Neolithic revolution. Although it is broadly accepted that this also applies to measles, the exact date of emergence for this disease is controversial. We sequenced the genome of a 1912 measles virus and used selection-aware molecular clock modeling to determine the divergence date of measles virus and rinderpest virus. This divergence date represents the earliest possible date for the establishment of measles in human populations. Our analyses show that the measles virus potentially arose as early as the sixth century BCE, possibly coinciding with the rise of large cities.

Measles is a highly contagious viral disease that presents with rash, fever, and respiratory symptoms. Before a live-attenuated vaccine was developed in the 1960s, the disease affected the vast majority of children (*1*, *2*). Global vaccination campaigns resulted in a marked reduction of measles transmission and fatal cases, and the World Health Organization (WHO) has proclaimed an elimination goal. However, the disease still caused an estimated 110,000 deaths in 2017 (*3*), and incidence has recently been on the rise (*4*). Measles is caused by *Measles morbillivirus* (MeV), a negative-sense single-stranded RNA virus from the family *Paramyxoviridae* (Order: *Mononegavirales*). MeV is an exclusively human pathogen whose closest relative was the now eradicated *Rinderpest morbillivirus* (RPV), a devastating cattle pathogen (*5*). It is generally accepted that measles emergence resulted from a spillover from cattle to humans, although the directionality of this cross-species transmission event has never been formally established (supplementary text S1) (*6*).

It is unclear when measles first became endemic in human populations, but assuming an origin in cattle, the earliest possible date of MeV emergence is defined by the MeV-RPV divergence time. Several studies have provided estimates for this date using molecular-clock analyses (*7*–*10*), with the most reliable (and oldest) estimate falling at the end of the ninth century CE {mean, 899 CE [95% highest posterior density (HPD) interval, 597 to 1144 CE]} (*8*). We reassessed the MeV-RPV divergence time using advanced, selection-aware Bayesian molecular-clock modeling (*11*) on a dataset of heterochronous MeV genomes, including the oldest human RNA virus genome sequenced to date, and show that a considerably earlier emergence can no longer be excluded.

Our reexamination was prompted by the broadly accepted view that molecular dating based on tip date calibration—the method used in previous efforts to estimate the timing of MeV-RPV divergence—underestimates deep divergence times (*8*). Rapid short-term substitution rates captured with tip date calibration often cannot be applied over long evolutionary time scales because of the effects of long-term purifying selection and substitution saturation. This causes a discrepancy between short- and long-term substitution rates, which is referred to as the time-dependent rate phenomenon (*12*, *13*). Because measurement time scales matter, a first step to arrive at accurate estimates is to maximize the time depth of tip date calibration—for example, through the use of ancient viral sequences (*14*, *15*).

RNA tends to be much less stable in the environment than DNA, making the recovery of MeV genetic material from archaeological remains unlikely (*16*). Pathology collections represent a more realistic source of MeV sequences that predate the oldest MeV genome: the genome of the Edmonston strain that was isolated in 1954 and attenuated to become the first measles vaccine. We examined a collection of lung specimens gathered by Rudolf Virchow and his successors between the 1870s and 1930s and preserved by the Berlin Museum of Medical History at the Charité (Berlin, Germany) and identified a 1912 case diagnosed with fatal measles-related bronchopneumonia (Fig. 1, fig. S1, and supplementary text S2 and S3). To retrieve MeV genetic material from this specimen, we first heat-treated 200 mg of the formalin-fixed lung tissue to reverse macromolecule cross-links induced by formalin and subsequently performed nucleic acid extraction (*17*). After deoxyribonuclease treatment and ribosomal RNA depletion, we built high-throughput sequencing libraries and shotgun sequenced them on Illumina platforms. We generated 27,328,219 high-quality reads, of which 0.46% were mapped to a MeV genome. Median insert size varied between 95 and 136 nucleotides (nt), and little damage was observed, suggesting good preservation of RNA molecules (fig. S2, table S1, and supplementary text S4). The resulting 10,960 unique MeV reads allowed us to reconstruct an almost complete 1912 MeV genome: 15,257 of the 15,894 nt in the MeV strain Edmonston (AF266288) were covered by at least three unique reads (11,988 nt by at least 20 reads; mean coverage 54x).

In addition to the 1912 genome and the 1954 Edmonston genome, only two genomes have been determined from MeV isolated before 1990 (Mvi/Lyon.FRA/77, HM562899; and T11wild, AB481087). We therefore searched the strain collection of the German National Reference Laboratory (Robert Koch Institute, Berlin, Germany) for pre-1990 isolates. We found two strains from the pre-vaccine era isolated in 1960 by the National Reference Laboratory of former Czechoslovakia in Prague (MVi/Prague.CZE/60/1 and MVi/Prague.CZE/60/2) (*18*). We performed serial passages of these strains and determined their genome sequences at a mean coverage of 109x and 70x, respectively. The two genomes were nearly identical, differing at only four sites.

We performed Bayesian and maximum likelihood (ML) phylogenetic analyses to investigate the phylogenetic placement of the 1912 and 1960 genomes with respect to 127 available MeV genomes. Tip-dated Bayesian phylogenetic trees placed the 1912 genome as a sister lineage to all modern genomes, whereas the two genomes from 1960 clustered together with the Edmonston strain (genotype A) (fig. S3). The placement of the 1912 genome in the dated-tip tree was consistent with its placement in a non-clock ML tree reconstruction and with the rooting of a dated-tip tree excluding the 1912 genome (fig. S4 A and B). The relatedness of the 1912 and 1960 genomes to now extinct MeV lineages is in line with a

[1]Epidemiology of Highly Pathogenic Microorganisms Project Group, Robert Koch Institute, Berlin, Germany. [2]Viral Evolution Project Group, Robert Koch Institute, Berlin, Germany. [3]Laboratory of Clinical and Evolutionary Virology, Department of Microbiology, Immunology and Transplantation, Rega Institute, Katholieke Universiteit (KU) Leuven, Leuven, Belgium. [4]Institute for Pathology, Charité, Berlin, Germany. [5]Département de Biologie, Ecole Normale Supérieure, PSL Université Paris, Paris, France. [6]National Reference Centre for Measles, Mumps, and Rubella, Robert Koch Institute, Berlin, Germany. [7]Department of Biostatistics, Fielding School of Public Health, University of California, Los Angeles, Los Angeles, CA, USA. [8]Department of Biomathematics, David Geffen School of Medicine, University of California, Los Angeles, Los Angeles, CA, USA. [9]Department of Human Genetics, David Geffen School of Medicine, University of California, Los Angeles, Los Angeles, CA, USA. [10]Berlin Museum of Medical History, Charité, Berlin, Germany. [11]Department of Classics and Letters, University of Oklahoma, Norman, OK, USA.
*These authors contributed equally to this work. †These authors contributed equally to this work.
‡Corresponding author. Email: calvignacs@rki.de

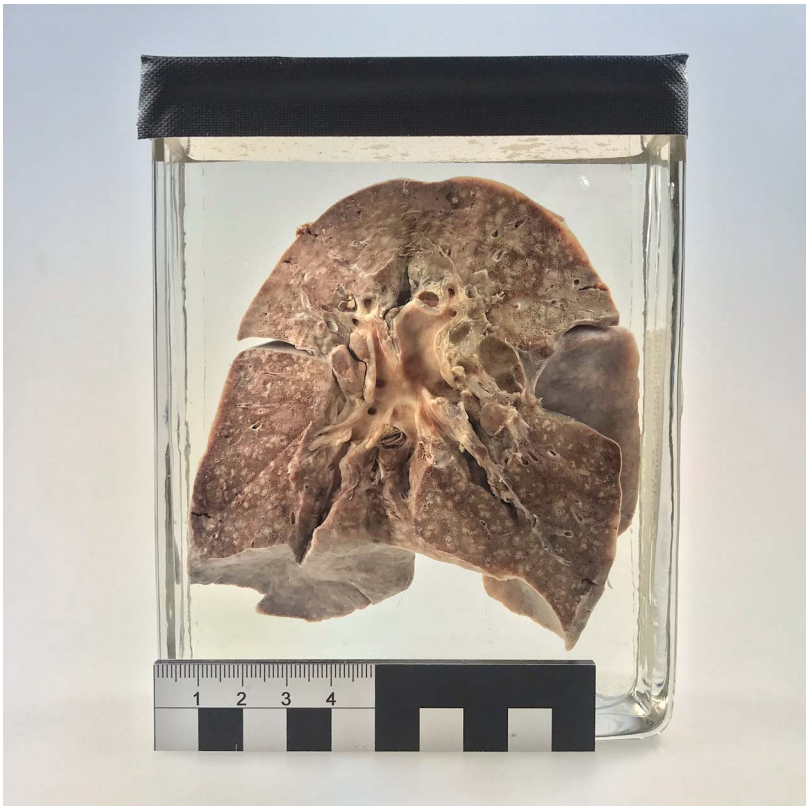

Fig. 1. Formalin-fixed lung specimen collected in 1912 in Berlin. Specimen is from a 2-year-old girl diagnosed with measles-related bronchopneumonia (museum object ID: BMM 655/1912).

marked reduction of MeV genetic diversity during the 20th century as a product of massive vaccination efforts.

Having extended the depth of MeV tip date calibration, we subsequently focused our attention on estimating the timing of MeV-RPV divergence. We assembled a dataset of 51 genomes comprising MeV (including one of the 1960 genomes and the 1912 genome), RPV, and Peste des petits ruminants virus (PPRV; the closest relative to MeV-RPV) sequences, ensuring that they represented the known genetic diversity of these viruses (table S2). Before inferring a time-scaled evolutionary history for this dataset by using a Bayesian phylogenetic framework, we assessed its temporal signal and tested it for substitution saturation. We confirmed a strong temporal signal (fig. S5 and table S3) and did not identify strong substitution saturation (table S4). We constructed a series of increasingly complex evolutionary models to accommodate various sources of rate heterogeneity. Models ranged from a standard codon substitution model with a strict molecular clock assumption to a codon substitution model with time-varying selection combined with a clade-specific rate for PPRV and additional branch-specific random effects on the substitution rate. Adequately accommodating different sources of rate heterogeneity is known to provide a better correction for multiple hits in genetic distance estimation,

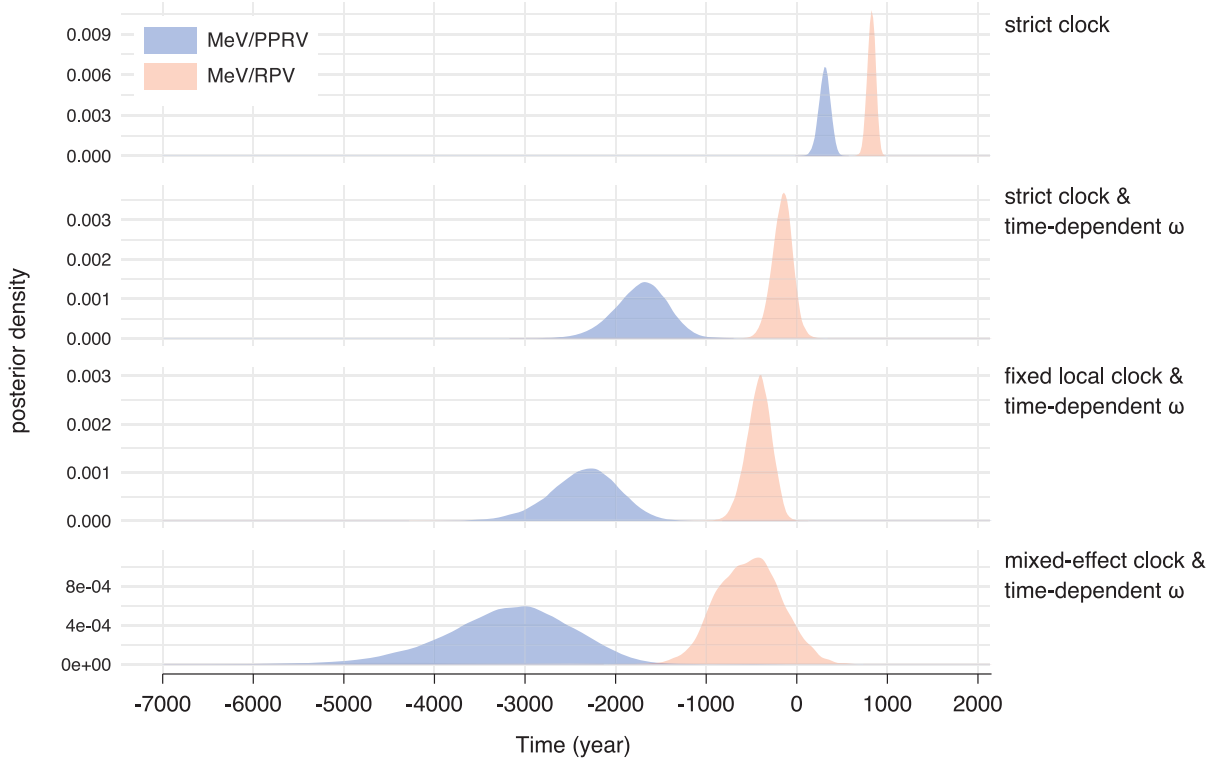

Fig. 2. Divergence time estimates for MeV and RPV (red) and for MeV-RPV and PPRV (blue) under increasingly complex evolutionary models. Estimates for parameters of interest (posterior mean and 95% highest posterior density interval) under each model are provided in table S5.

and the potential of codon substitution modeling in recovering deep viral divergence has been demonstrated specifically (*8*). This was reflected in the increasingly older estimates of MeV-RPV and PPRV-MeV-RPV divergence times and wider credible intervals for increasingly complex models (Fig. 2 and table S5). Parameter estimates of the substitution and clock models also provided evidence for a significant contribution of these different sources of rate heterogeneity to model fit improvement (table S5). We found a significantly negative coefficient for the time-dependent nonsynonymous/synonymous substitution rate ratio (ω) (*11*), indicating strong long-term purifying selection; a significantly positive coefficient for the fixed effect on the PPRV rate, indicating a faster evolutionary rate in this clade (as suggested by temporal signal analyses, fig. S5); and significant additional unexplained variation, as modeled by the random effects (table S5). Our most complex model therefore provided the best description of the evolutionary process and pushed back the divergence date of MeV and RPV, with a mean estimate at 528 BCE (95% HPD interval, 1174 BCE to 165 CE) (Fig. 3). These estimates were robust to (i) including or excluding the 1912 genome in the analyses (table S6), (ii) using a more conservative consensus genome for the 1912 sample (table S7), (iii) the prior specification on the age of the RPV genome or the inclusion of an additional RPV genome (table S7), and (iv) the coalescent prior specification (table S7). A comparison of the four models in their ability to recover the age of the 1912 genome indicated that the most complex model yielded the best estimate [1929 CE (95% HPD interval, 1889 to 1961 CE)] (fig. S6).

The MeV-RPV divergence time provides the earliest possible date for measles emergence in humans, which is now compatible with the emergence of this disease more than 2500 years ago. It seems plausible that the divergence of these lineages was closely followed by the cattle-to-human host jump and subsequent evolution into two distinct pathogens. However, the spillover could have occurred at any time between the MeV-RPV divergence and the time to the most recent common ancestor of all MeV known to infect humans [1880 CE (95% HPD interval, 1865 to 1893 CE)]. This raises the question of whether other sources of information can narrow down this time frame and agree with an earlier timing of measles emergence.

The earliest clear clinical description of measles is often attributed to the Persian physician Rhazes, writing in the 10th century CE (*19*). But Rhazes was extremely familiar with all available medical literature at his time and made use of earlier sources. Indian medical texts possibly describe measles several centuries before Rhazes (*20*). Although clear descriptions of measles are missing in the Hippocratic corpus and the Greek medical tradition (at least through the prolific second-century writer Galen), such absence alone cannot be decisive. Retrospective diagnosis from premodern medical texts is notoriously fraught, especially for diseases such as measles, whose symptoms were easily confused with a variety of other conditions. Measles differential diagnosis remained a challenge well into more recent times (*21*). Therefore, any number of the large-scale "pestilences" described in ancient sources from Europe or China could reflect MeV outbreaks.

An ancient origin of measles seems all the more plausible in the light of demographic changes that are compatible with our understanding of (contemporary) MeV epidemiology. Populations large enough to support continuous MeV transmission—larger than the MeV critical community size (CCS) of 250,000 to 500,000 individuals (*22*–*24*)—could not exist in Neolithic, Bronze Age, and early Iron Age settlements, which lacked both economic and political means to allow such numbers. Even if connectivity between such settlements may have created a larger pool of susceptible individuals, epidemiologists have held that given the speed with which measles epidemics occur and the efficacy of acquired immunity, MeV could not have become endemic in urban populations below the CCS (*25*). In the late first millennium BCE, technologies (both economic and political) crossed a threshold, promoting an upsurge in population sizes in Eurasia and South and East Asia. Although considerable uncertainty exists around population size estimates derived from ancient documents (for

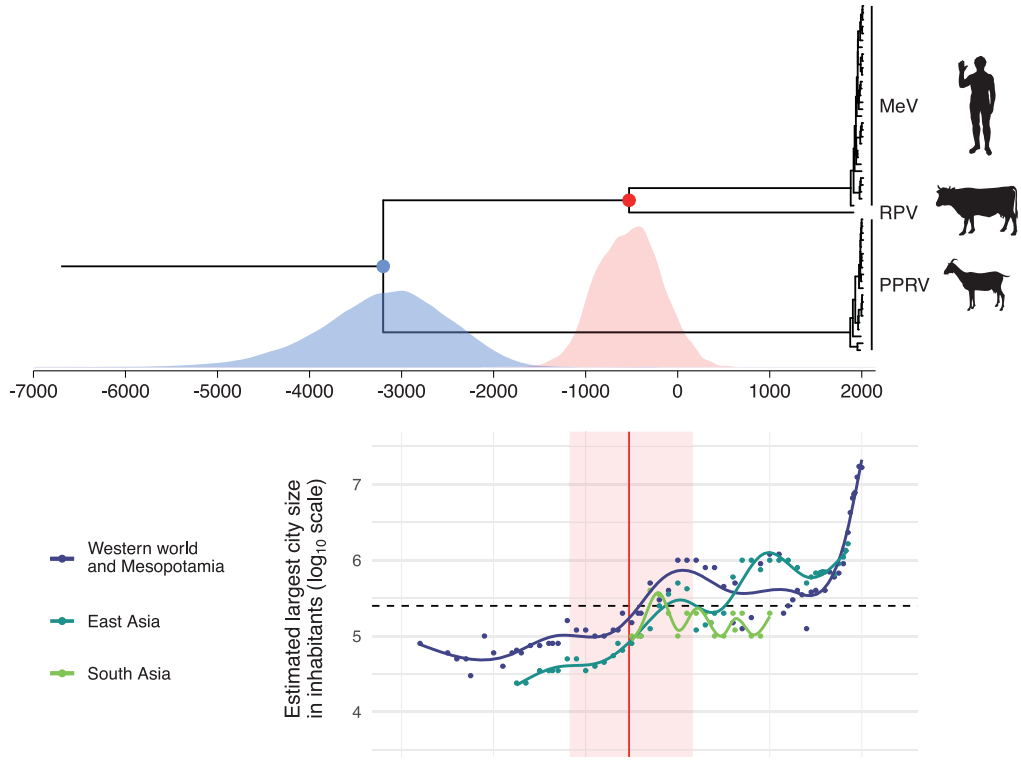

Fig. 3. Time-measured evolutionary history for MeV, RPV, and PPRV and largest city size over time in three well-studied regions of the world. (**Top**) Maximum clade credibility tree summarized from a Bayesian time-measured inference by using tip-dating and accounting for long-term purifying selection. The red and blue points represent the mean estimates for the divergence times between MeV and RPV then MeV-RPV and PPRV, respectively; the corresponding divergence date estimates are depicted below as marginal posterior distributions. (**Bottom**) The estimated size (log10 scale) of the largest city in the western world including Mesopotamia (dark blue), East Asia (dark green), and South Asia (green) over time. The red vertical line indicates the mean divergence time estimate between MeV and RPV, and the red area indicates its 95% highest posterior density interval. The dashed horizontal line represents the classical threshold for MeV maintenance in a population (250,000 individuals). Dots show data points according to Morris (*34*) and Inoue *et al*. (*26*). Each line represents the fit of a generalized additive model with a cubic spline smoothing function.

example, literary observations, travelers' reports, censuses, or references to the amount of food distributed in a city) or archaeological proxies (such as the size of city walls or a built-up area of settlement), there is broad agreement that a number of settlements in North Africa, India, China, Europe, and the Near East began to surpass the CCS for MeV by around 300 BCE, presumably for the first time in human history (Fig. 3) (*26*). From this period onward, there were consistently urban populations above the CCS for MeV.

On the basis of these considerations, our substantially older MeV-RPV divergence estimate provides grounds for sketching a new model of MeV's evolutionary history. Under this scenario, a bovine virus, the common ancestor of modern strains of RPV and MeV, circulated in large populations of cattle (and possibly wild ungulates) since its divergence from PPRV around the fourth millennium BCE [3199 BCE (95% HPD interval, 4632 to 1900 BCE)] (Fig. 3). As a fast-evolving RNA virus, it may have produced variants that were able to cross the species barrier on several occasions, but small human populations could only serve as dead-end hosts. Then, almost as soon as contiguous settlements reached sufficient sizes to maintain the virus' continuous transmission (Fig. 3), it emerged as a human pathogen, the progenitor of modern-day MeV. It has been suggested that numerous concurrent human-bovine epidemics in the early medieval period (here, 6th to 10th centuries CE) were caused by an immediate ancestor of MeV and RPV that was pathogenic to both cattle and humans (*27*). The new MeV-RPV divergence date allows for the same inference to be made for earlier concurrent human-bovine mortality events well attested in, for example, Roman sources from the fifth century BCE on (*28*). During the following centuries, introduction of MeV into naive human populations and/or flare-ups of the disease might have caused some ancient epidemics whose etiology remains uncertain.

Although our findings shed new light on the origin of measles, formally proving that the virus emerged soon after its divergence from RPV would require archaeological genomic evidence. Most studies on ancient viruses have thus far focused on viruses with a double-stranded DNA genome (*14*, *29*–*32*). However, genetic material of parvovirus B19 was also detected in early Neolithic skeletal remains, despite the relatively unstable nature of its single-stranded DNA genome (*15*). It remains to be determined whether viral RNA recovery from such ancient specimens is feasible. Recently, RNA was extracted from the remains of a 14,300-year-old Pleistocene canid preserved in permafrost (*33*). Although the majority of RNA fragments were extremely short (<30 nt), the authenticity of the sequences could be validated (*33*). Such advances highlight that it may not be completely impossible for ancient remains to still contain MeV RNA, especially if preserved under favorable circumstances, including natural mummification or preservation in cold environments (*16*). While awaiting such direct evidence, we believe that the proposed model of MeV evolution constitutes a compelling working hypothesis.

REFERENCES AND NOTES

1. A. D. Langmuir, *Am. J. Dis. Child.* **103**, 224–226 (1962).
2. W. J. Moss, *Lancet* **390**, 2490–2502 (2017).
3. A. Dabbagh *et al.*, *MMWR Morb. Mortal. Wkly. Rep.* **67**, 1323 (2018).
4. WHO, Provisional data based on monthly data reported to WHO (Geneva) as of January 2020; www.who.int/immunization/monitoring_surveillance/burden/vpd/surveillance_type/active/measles_monthlydata/en
5. P. Roeder, J. Mariner, R. Kock, *Philos. Trans. R. Soc. Lond. B Biol. Sci.* **368**, 20120139 (2013).
6. N. D. Wolfe, C. P. Dunavan, J. Diamond, *Nature* **447**, 279–283 (2007).
7. Y. Furuse, A. Suzuki, H. Oshitani, *Virol. J.* **7**, 52 (2010).
8. J. O. Wertheim, S. L. Kosakovsky Pond, *Mol. Biol. Evol.* **28**, 3355–3365 (2011).
9. M. Muniraju *et al.*, *Emerg. Infect. Dis.* **20**, 2023–2033 (2014).
10. H. Kimura *et al.*, *Sci. Rep.* **5**, 11648 (2015).
11. J. V. Membrebe, M. A. Suchard, A. Rambaut, G. Baele, P. Lemey, *Mol. Biol. Evol.* **36**, 1793–1803 (2019).
12. S. Y. Ho, S. Duchêne, M. Molak, B. Shapiro, *Mol. Ecol.* **24**, 6007–6012 (2015).
13. P. Aiewsakun, A. Katzourakis, *J. Virol.* **90**, 7184–7195 (2016).
14. B. Mühlemann *et al.*, *Nature* **557**, 418–423 (2018).
15. B. Mühlemann *et al.*, *Proc. Natl. Acad. Sci. U.S.A.* **115**, 7557–7562 (2018).
16. O. Smith, M. T. Gilbert, in *Paleogenomics: Genome-Scale Analysis of Ancient DNA*, C. Lindqvist, O. P. Rajora, Eds. (Springer, 2019).
17. M. T. Gilbert *et al.*, *PLOS ONE* **2**, e537 (2007).
18. S. Santibanez, A. Heider, E. Gerike, A. Agafonov, E. Schreier, *J. Med. Virol.* **58**, 313–320 (1999).
19. R. Kim-Farley, in *The Cambridge World History of Human Disease*, K. F. Kiple, Ed. (Cambridge Univ. Press, 1993).
20. K. R. L. Gupta (translator), *Madhava Nidana: Ayurvedic System of Pathology* (Sri Satguru Publications, 1987).
21. B. A. Cunha, *Infect. Dis. Clin. North Am.* **18**, 79–100 (2004).
22. M. S. Bartlett, *J. R. Stat. Soc. [Ser A]* **120**, 48–70 (1957).
23. F. L. Black, *J. Theor. Biol.* **11**, 207–211 (1966).
24. M. J. Keeling, B. T. Grenfell, *Science* **275**, 65–67 (1997).
25. A. D. Cliff, P. Haggett, M. Smallman-Raynor, *Measles: An Historical Geography of a Major Human Viral Disease: From Global Expansion to Local Retreat, 1840–1990* (Blackwell, 1993).
26. H. Inoue *et al.*, *Soc. Sci. Hist.* **39**, 175–200 (2015).
27. T. P. Newfield, *J. Interdiscip. Hist.* **46**, 1–38 (2015).
28. C. A. Spinage, *Cattle Plague: A History* (Springer, 2003).
29. P. Biagini *et al.*, *N. Engl. J. Med.* **367**, 2057–2059 (2012).
30. A. T. Duggan *et al.*, *Curr. Biol.* **26**, 3407–3412 (2016).
31. Z. Patterson Ross *et al.*, *PLOS Pathog.* **14**, e1006750 (2018).
32. B. Krause-Kyora *et al.*, *eLife* **7**, e36666 (2018).
33. O. Smith *et al.*, *PLOS Biol.* **17**, e3000166 (2019).
34. I. Morris, *The Measure of Civilization: How Social Development Decides the Fate of Nations* (Princeton Univ. Press, 2013).
35. S. Lequime, slequime/measles-history: Publication. Zenodo (2020); doi: 10.5281/zenodo.3764907.

ACKNOWLEDGMENTS

The 1912 MeV genome was generated from a formalin-fixed lung specimen (museum object ID: BMM 655/1912) from the collection of the Berlin Museum of Medical History at the Charité (Berlin, Germany). Ethics approval was obtained from the ethics committee of the Charité (Berlin, Germany) under the reference number EA4/212/19. We thank the National Institute of Public Health, Prague, Czech Republic, for providing us with the MeV strains MVi/Prague.CZE/60/1 and MVi/Prague.CZE/60/2 and O. Smith and J. Wertheim for helpful suggestions. The Titan V GPU used for this research was donated by the NVIDIA Corporation. **Funding:** The research leading to these results has received funding from the European Research Council under the European Union's Horizon 2020 research and innovation program (grant agreement ~725422-ReservoirDOCS). P.L. acknowledges support by the Research Foundation–Flanders ('Fonds voor Wetenschappelijk Onderzoek–Vlaanderen,' FWO: G066215N, G0D5117N, and G0B9317N). S.L. and B.V. are postdoctoral research fellows funded by the FWO. M.A.S. was partially supported through National Institutes of Health grant U19 AI135995. **Author contributions:** Conceptualization: P.L. and S.C.-S.; data curation: A.D., S.L., B.V., M.A.S., P.L., and S.C.-S.; formal analysis: A.D., S.L., B.V., J.F.G., M.U., P.L., and S.C.-S.; funding acquisition: F.H.L. and S.C.-S.; investigation: A.D., L.V.P., S.B., A.H., D.H., K.M., B.P., and J.S.; methodology: S.L., B.V., M.A.S., and P.L.; project administration: F.H.L., P.L., and S.C.-S.; resources: S.S., N.W., A.M., F.H.L., T.S., P.L., and S.C.-S.; software: S.L., B.V., M.A.S., and P.L.; supervision: P.L. and S.C.-S.; validation: A.D., M.U., J.F.G., and S.C.-S.; visualization: S.L.; writing, original draft: A.D., S.L., K.H., P.L., and S.C.-S.; writing, review and editing: all authors. **Competing interests:** All authors declare no competing interests. **Data and materials availability:** The sequencing data for this study have been deposited in the European Nucleotide Archive (ENA) at the European Molecular Biology Laboratory–European Bioinformatics Institute under accession no. PRJEB36265 (www.ebi.ac.uk/ena/data/view/PRJEB36265). Human reads have been removed from 1912 sequencing files before uploading (supplementary materials). Alignments, trees, and BEAST xml files are available at https://github.com/slequime/measles-history (*35*).

SUPPLEMENTARY MATERIALS

science.sciencemag.org/content/368/6497/1367/suppl/DC1
Materials and Methods
Supplementary Text S1 to S4
Figs. S1 to S6
Tables S1 to S7
References (*36*–*83*)

View/request a protocol for this paper from *Bio-protocol*.

17 January 2020; accepted 30 April 2020
10.1126/science.aba9411

Science

Measles virus and rinderpest virus divergence dated to the sixth century BCE

Ariane Düx, Sebastian Lequime, Livia Victoria Patrono, Bram Vrancken, Sengül Boral, Jan F. Gogarten, Antonia Hilbig, David Horst, Kevin Merkel, Baptiste Prepoint, Sabine Santibanez, Jasmin Schlotterbeck, Marc A. Suchard, Markus Ulrich, Navena Widulin, Annette Mankertz, Fabian H. Leendertz, Kyle Harper, Thomas Schnalke, Philippe Lemey and Sébastien Calvignac-Spencer

Science **368** (6497), 1367-1370.
DOI: 10.1126/science.aba9411

Older origins of measles virus

Animal domestication by humans is thought to have given many pathogens an opportunity to invade a new host, and measles is one example of this. However, there is controversy about when measles emerged in humans, because the historical descriptions of measles are relatively recent (late ninth century CE). The controversy has persisted in part because ancient RNA is thought to be a poor target for molecular clock techniques. Düx *et al.* have overcome the ancient RNA challenge by sequencing a measles virus genome obtained from a museum specimen of the lungs of child who died in 1912 (see the Perspective by Ho and Duchêne). The authors used these and other more recent sequencing data in a Bayesian molecular clock–modeling technique, which showed that measles virus diverged from rinderpest virus in the sixth century BCE, indicating an early origin for measles possibly associated with the beginnings of urbanization.

Science, this issue p. 1367; see also p. 1310

Science (print ISSN 0036-8075; online ISSN 1095-9203) is published by the American Association for the Advancement of Science, 1200 New York Avenue NW, Washington, DC 20005. The title *Science* is a registered trademark of AAAS.